

## Voltammetric Study on the Electrowinning of Cobalt in the Presence of Additives

Danielle C. de Castro,<sup>✉\*</sup><sup>a</sup> Iranildes D. dos Santos,<sup>✉<sup>b</sup></sup> Marcelo B. Mansur<sup>a</sup> and Achilles J. B. Dutra<sup>✉<sup>a</sup></sup>

<sup>a</sup>Programa de Pós-Graduação em Engenharia Metalúrgica e de Materiais, COPPE, Universidade Federal do Rio de Janeiro (UFRJ), Av. Horácio Macedo, 2030, Cidade Universitária, 21941-914 Rio de Janeiro-RJ, Brazil

<sup>b</sup>Instituto Tecnológico Vale (ITV), Rua Prof. Paulo Magalhães Gomes, s/n, Morro do Cruzeiro, 35400-000 Ouro Preto-MG, Brazil

Cobalt electrowinning is an intensive energy-consuming process, and allied to the increasing demand for pure cobalt, has led to the need for optimization. Based on a statistical approach, the effects of additives, including sodium lauryl sulfate (SLS), boric acid ( $H_3BO_3$ ), and cobalt chloride ( $CoCl_2$ ) on the current efficiency of electrowinning have been studied using the cyclic voltammetry (CV). CV tests indicated the concentration range of the more appropriate additives to be used in the factorial design study of electrowinning. Regarding the electrowinning tests, the addition of  $0.05\text{ g L}^{-1}$  SLS,  $10\text{ g L}^{-1}$   $H_3BO_3$ ,  $50\text{ g L}^{-1}$   $Na_2SO_4$ , and  $1\text{ g L}^{-1}$   $CoCl_2$  led to a current efficiency of 96% and energy consumption of  $1.95\text{ kWh kg}^{-1}$ , along with a smooth metallic deposit without evident pits and other defects. SLS in its higher concentration level led to the formation of compact structures, while the higher concentration level of  $H_3BO_3$ , lightens the deposits.

**Keywords:** cyclic voltammetry, electrowinning, cobalt metal, additive

### Introduction

Cobalt is a strategic metal that is mostly used to produce batteries, super alloys, catalysts, etc., and its supply depends on the global economic scenario of nickel (Ni) and copper (Cu) since 95% of cobalt is obtained as a by-product of Cu and Ni mining.<sup>1,2</sup> The largest exporter of concentrated cobalt in the world is the Democratic Republic of Congo. However, in terms of high-value-added cobalt production, China has been the leader over the last few years, importing around US\$2.23 billion of cobalt in 2018.<sup>3,4</sup> This fact was due to the manufacture of rechargeable batteries for electric vehicles (EVs).

Due to an increasing trend in the production of EVs, the demand for cobalt has increased during the last five years.<sup>5-8</sup> Recently, Dehaine *et al.*<sup>2</sup> reported an expressive growth of cobalt prices since 2020, reaching US\$ 80,000 *per ton*, after a peak in March of 2018 (ca. 93,000 *per ton*). In this context, the extractive metallurgical industries directed their investments toward cobalt recovery processes, including electrowinning.<sup>9</sup>

Electrowinning is considered an expensive process because it requires considerable electric energy to produce metal deposits with technologically acceptable physical and chemical properties.<sup>10</sup> One ton of cobalt metal requires approximately 5,300 kWh *per ton* of energy.<sup>5</sup> Nevertheless, there is still a growing need to produce Co-materials nowadays, due to their applications in the production of cobalt-bearing superalloys, which corresponds to the second largest single end-use of cobalt, while the first, the rechargeable batteries, corresponds to 58% of its applications.<sup>2</sup> Reducing the cobalt electrowinning's operational costs and energy consumption is paramount.

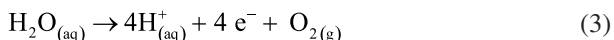
Cyclic voltammetry (CV) is a powerful technique that can provide useful information about electrochemical reactions mechanism, electrolysis parameters, the kinetics of heterogeneous electron transport reactions, and coupled chemical reactions on electrodes.<sup>11</sup> In addition, it allows to estimate the current efficiency of some electrolytic reactions through the ratio of oxidation and reduction charges, obtained through the areas of current *versus* time graphs of the direct and reverse potential sweeps.<sup>12,13</sup>

Concerning cobalt electrowinning, additives can influence the hydrogen bubbles generation on the cathode, the reduction rate of  $Co^{2+}$  ions, and the pH at the electrode/

\*e-mail: danielle.costal@coppe.ufrj.br

Editor handled this article: Rodrigo A. A. Muñoz (Associate)

electrolyte interface. Equations 1 and 2 are the cobalt electrowinning cathodic reactions, while equation 3 is the anodic reaction. The reduction of  $\text{Co}^{2+}$  ions occurs concomitantly with the reduction of  $\text{H}^+$  ions, which is the main side-reaction during cobalt electrowinning.



The presence of additives during the electrodeposition is important to reduce the detrimental effects of hydrogen bubbles on the metallic deposit, leading to a cobalt metal deposit with superior quality, including its brightness, grain size reduction, and smoothness.<sup>14</sup> However, the effect of additives is commonly studied individually,<sup>14-17</sup> and the interaction among the additives is generally omitted.

Some studies<sup>1,18,19</sup> indicate that the adequate introduction of chloride ions and certain organic compounds are considered important factors to control the morphology of the deposit, preventing the formation of dendritic structures. The addition of these species must be in a narrow concentration range because, when present in lower or higher amounts, they become undesirable due to the formation of free chlorine on the anode, cathode contamination, and other detrimental effects.

Sodium lauryl sulfate (SLS) can also affect the morphology of Co deposits. SLS, as a surfactant, decreases the superficial tension on the interface electrode/hydrogen gas. Consequently, it favors the release of hydrogen gas bubbles formed on the cathode avoiding the formation of pits on the metal deposit.<sup>20-22</sup>

Another additive that can act at the electrode-electrolyte interface is boric acid ( $\text{H}_3\text{BO}_3$ ).  $\text{H}_3\text{BO}_3$  is a known pH buffer for acidic solutions and its concentration, under different conditions, has been investigated by several authors.<sup>20,23,24</sup> Santos *et al.*<sup>25</sup> reported that the reduction of  $\text{H}^+$  ions concentration in the cathode vicinity can lead to a predominance of hydroxylated species of cobalt on the working electrode. Tripathy and Muir<sup>26</sup> observed that boric acid raised current efficiency by 2 to 3% and decreased energy consumption.

Hence, this paper aims to apply cyclic voltammetry (CV) as a rapid response tool to investigate the effect of additives for cobalt electrowinning. Those CV results were used to plan a factorial design to study the synergistic effect of some common additives on the current efficiency and specific energy consumption for 6 h electrowinning tests. In

addition, the relationship between additives and the quality of cobalt deposits was also investigated.

## Experimental

CV tests were used to determine the lower and higher concentration levels to be tested in long-duration electrowinning tests. A Autolab/PGSTAT204 potentiostat (Metrohm, São Paulo, Brazil) was used to run the voltametric experiments. Then, a 2<sup>4</sup> factorial design was elaborated to study the synergistic effect of some common additives for cobalt electrowinning. The variables under investigation were: SLS,  $\text{H}_3\text{BO}_3$ ,  $\text{Na}_2\text{SO}_4$ , and  $\text{CoCl}_2$  concentrations.

The response variables of the statistical factorial design were current efficiency and specific energy consumption. The morphology and purity of the obtained deposits were analyzed by scanning electron microscopy (SEM), coupled with energy dispersion spectroscopy (EDS) (TESCAN VEGA3<sup>®</sup>/D-12489 model, Brno, Czech Republic). Additionally, macrophotographs were obtained with an Avantscope<sup>®</sup> digital microscope (Avantscope<sup>®</sup>, São Paulo, Brazil).

### Influence of additives on the cyclic voltammograms

For cyclic voltammetry tests, a synthetic electrolyte solution of heptahydrate cobalt sulfate (min. 99%, Isofar, Duque de Caxias, Brazil), with 60 g L<sup>-1</sup> of  $\text{Co}^{2+}$  ions, was prepared and only one additive was introduced *per* test, at the indicated concentration. The additives composition range of the electrolyte for the cyclic voltammograms is presented in Table 1.

**Table 1.** Additives composition range of the electrolyte for the cyclic voltammograms

| Additive   | Concentration / (g L <sup>-1</sup> ) |
|--|--------------------------------------|
| $\text{H}_3\text{BO}_3$ (min. 99%, Biograde, San Francisco, USA)         | 10 to 70                             |
| $\text{Na}_2\text{SO}_4$ (min. 99%, Vetec LTDA, Duque de Caxias, Brazil) | 50 to 100                            |
| SLS (min. 85%, Biograde, San Francisco, USA)                             | 0.01 to 0.05                         |
| $\text{CoCl}_2$ (min. 99%, Biograde, San Francisco, USA)                 | 1.0 to 30.0                          |

SLS: sodium lauryl sulfate.

The pH, temperature, and values of  $\text{Co}^{2+}$  ion concentration for cobalt electrowinning were previously selected according to studies conducted by Passos *et al.*,<sup>27</sup> Sharma *et al.*<sup>28</sup> and Elsherief.<sup>29</sup> Thus, a cobalt sulfate solution with 60 g L<sup>-1</sup> of  $\text{Co}^{2+}$  ions and pH equal to 4, with the presence of the additives, was transferred to a jacketed

cell heated by a thermostatic bath to 60 °C.

Cyclic voltammetry tests were performed in a 3-electrodes jacketed cell with a volume of 200 mL. An AISI 304 stainless steel plate (with an exposed area of 0.386 cm<sup>2</sup>), a Ti/RuO<sub>2</sub> plate, and a saturated Ag/AgCl electrode have been used as working, counter, and reference electrodes, respectively. The scan rate was 20 mV s<sup>-1</sup>, from 0.0 to -0.8 and back to 0.0 V.

The results were presented as current density (mA cm<sup>-2</sup>) vs. potential (E) and current vs. time curves. From the area under the current vs. time curve, the electrical charge of the cathodic and anodic process was determined, allowing the estimation of current efficiency from the ratio of the integrals of the curves in the direction of oxidation and reduction, respectively. The areas were obtained through the integration of the graph performed in the Origin software® 9.0.<sup>30</sup> Equation 4 permits the current efficiency estimation (CE<sub>est</sub>) for the voltammetric tests and Figure 1 presents an example of the generated graphs with the respective cathodic and anodic charges.

$$CE_{est} = 100 \times \left| \frac{\text{anodic charge}}{\text{cathodic charge}} \right| \quad (4)$$

#### Cobalt electrowinning tests in a 2<sup>4</sup> factorial design experiment

The same concentration, temperature and pH conditions used in cyclic voltammetry tests were applied to electrowinning tests. Table 2 presents the additives concentration values selected for the factorial design experiments, which were chosen based on the best current efficiencies obtained during the cyclic voltammetry tests.

To evaluate the influence of the additive's concentration interactions, a 2<sup>4</sup> factorial design was performed with

the Minitab® 19 software,<sup>31</sup> in duplicate and with three replicates in medium point. Table 3 presents the design matrix of the experiments, according to Montgomery.<sup>32</sup>

**Table 2.** Additives concentration in the cobalt sulfate electrolyte factorial design experiments

| Additive                        | Minimum / (g L <sup>-1</sup> ) | Maximum / (g L <sup>-1</sup> ) | Medium point / (g L <sup>-1</sup> ) |
|---------------------------------|--------------------------------|--------------------------------|-------------------------------------|
| H <sub>3</sub> BO <sub>3</sub>  | 10                             | 30                             | 20                                  |
| Na <sub>2</sub> SO <sub>4</sub> | 50                             | 100                            | 75                                  |
| SLS                             | 0.02                           | 0.05                           | 0.03                                |
| CoCl <sub>2</sub>               | 1.0                            | 3.0                            | 2.0                                 |

SLS: sodium lauryl sulfate.

**Table 3.** 2<sup>4</sup> factorial design matrix of additives concentration for cobalt electrowinning experiments

| Run No. | Factor |   |   |   |
|---------|--------|---|---|---|
|         | A      | B | C | D |
| 1       | -      | - | - | - |
| 2       | +      | - | - | - |
| 3       | -      | + | - | - |
| 4       | +      | + | - | - |
| 5       | -      | - | + | - |
| 6       | +      | - | + | - |
| 7       | -      | + | + | - |
| 8       | +      | + | + | - |
| 9       | -      | - | - | + |
| 10      | +      | - | - | + |
| 11      | -      | + | - | + |
| 12      | +      | + | - | + |
| 13      | -      | - | + | + |
| 14      | +      | - | + | + |
| 15      | -      | + | + | + |
| 16      | +      | + | + | + |
| 17      | 0      | 0 | 0 | 0 |

The symbols “-”, “+” and “0” represent minimum, maximum and medium point concentration of additives, respectively. The A, B, C and D factors represent the additives: Na<sub>2</sub>SO<sub>4</sub>, CoCl<sub>2</sub>, SLS and H<sub>3</sub>BO<sub>3</sub>, respectively.

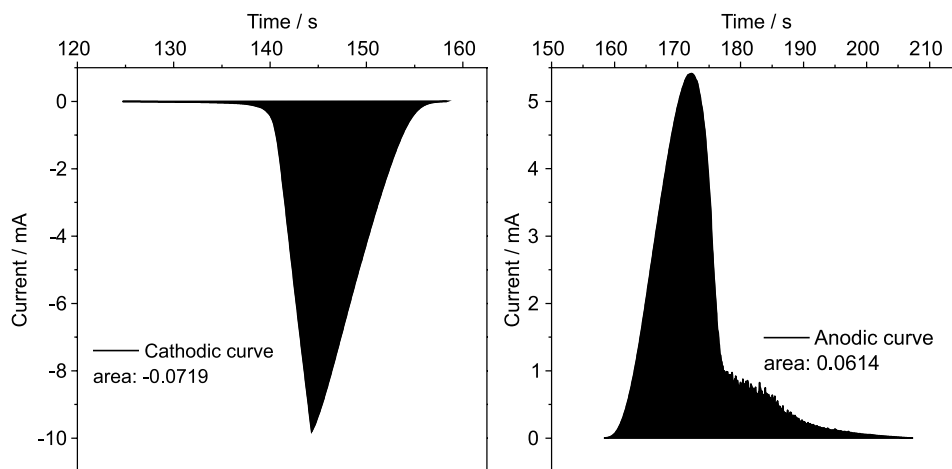


**Figure 1.** Current vs. time graph obtained from cyclic voltammetry for a CoSO<sub>4</sub> solution with 60 g L<sup>-1</sup> of Co<sup>2+</sup> ions and 0.03 g L<sup>-1</sup> of SLS, at 60 °C, pH 4 and scan rate of 20 mV s<sup>-1</sup>.

For the tests, a two-channel direct current source was used. The electrodes were an AISI 304 stainless steel with 0.386 cm<sup>2</sup> of active area, as a cathode, and Ti/RuO<sub>2</sub> plate, as an anode, which were placed 2.5 cm from each other. The current density applied was 200 A m<sup>-2</sup>.

The response variables obtained by the tests were the current efficiency and the specific energy consumption. The experiments were carried out during 6 h. The input variables were the concentrations of Na<sub>2</sub>SO<sub>4</sub> (A), CoCl<sub>2</sub> (B), SLS (C) and H<sub>3</sub>BO<sub>3</sub> (D).

The current efficiency (CE) and specific energy consumption (SEC) results obtained in the electrowinning were calculated according to equations 5 and 6, respectively:

$$CE = \frac{\text{mass obtained}}{\text{theoretical mass}} \quad (5)$$

$$SEC = I \times t \frac{V}{CE} \quad (6)$$

where V is the applied cell voltage and the product It is associated with the cell productivity by Faraday's law, where 1 eq-g of cobalt, theoretically, is deposited by a charge corresponding to 26.8 A h. The deposits mass was measured (after drying at 120 °C) with an analytical balance.

## Results and Discussion

### Effect of boric acid concentration (H<sub>3</sub>BO<sub>3</sub>)

The effect of boric acid concentration on the cyclic voltammograms for Co<sup>2+</sup> ions reduction on a stainless-steel electrode was followed by the dissolution of the deposited metal and is presented in Figure 2a. It can be

observed that the increase of H<sub>3</sub>BO<sub>3</sub> concentration in cobalt sulfate solutions causes a decrease in the current density value, mainly at concentrations higher than 30 g L<sup>-1</sup>, where a strong inhibition effect occurs, impairing cobalt deposition. Therefore, higher concentrations of H<sub>3</sub>BO<sub>3</sub> are not advantageous for Co electrowinning. Additionally, it was also observed that the increase of boric acid concentration raised cobalt nucleation overpotential and shifted the cobalt electrodeposition to more negative values.

The effect of boric acid on current efficiency is presented in Figure 2b. It is evident that the addition of H<sub>3</sub>BO<sub>3</sub> at up to 30 g L<sup>-1</sup> resulted in an increase of current efficiency, reaching 84%. On the other hand, a sharp drop in current efficiency (less than 70%) was observed for concentrations higher than 50 g L<sup>-1</sup>.

Zhou *et al.*<sup>19</sup> reported that 20 g L<sup>-1</sup> of boric acid concentration can buffer pH at the electrode/electrolyte interface vicinity preventing the formation of hydroxyl complexes, such as CoOH<sup>+</sup>. Tripathy *et al.*<sup>26</sup> also reported that the addition of boric acid polarizes cobalt deposition and increases its nucleation overpotential.

### Effect of sodium sulfate concentration (Na<sub>2</sub>SO<sub>4</sub>)

The effect of Na<sub>2</sub>SO<sub>4</sub> concentration on the cyclic voltammograms for cobalt deposition on stainless steel is presented in Figure 3a. It can be observed that the increase of Na<sub>2</sub>SO<sub>4</sub> concentration favors the increase of the current density, especially in the anodic branch, which corresponds to the redissolution of the cobalt, deposited along with hydrogen evolution, during the cathodic scan. Figure 3b indicates that the addition of 50 to 100 g L<sup>-1</sup> of Na<sub>2</sub>SO<sub>4</sub> promoted a smooth growth of current efficiency from 84 to 91%. According to Lu *et al.*<sup>20</sup> and Sharma *et al.*,<sup>28</sup>

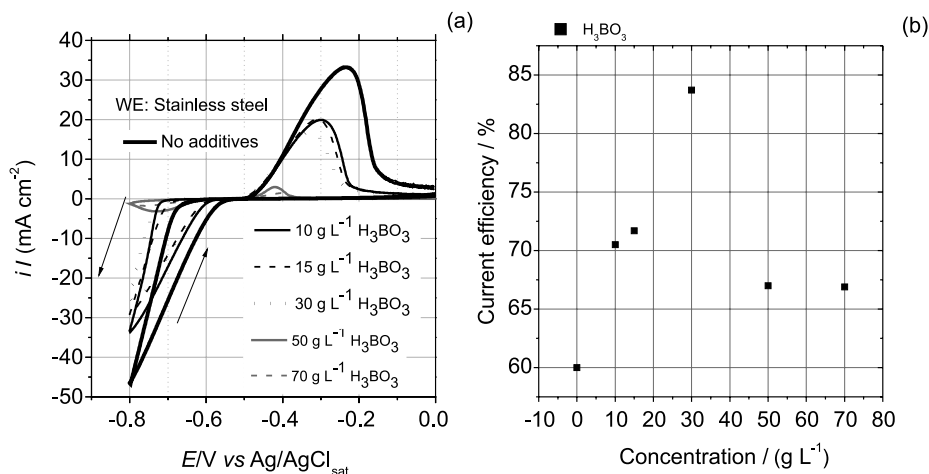


**Figure 2.** Effect of boric acid concentration on voltammograms (a) and (b) current efficiency in a CoSO<sub>4</sub> solution at 60 °C, pH 4, 60 g L<sup>-1</sup> of Co<sup>2+</sup> ions and scan rate 20 mV s<sup>-1</sup>.

sodium sulfate is characterized by increasing electrolyte conductivity, reducing the applied voltage necessary to achieve the desired current density generating less hydrogen evolution on the cathode. In fact, this increase in current efficiency can be attributed to a lower hydrogen ions activity, which favors cobalt deposition.

#### Effect of sodium lauryl sulfate concentration (SLS)

The effect of SLS concentration on the cyclic voltammograms for cobalt deposition and dissolution is presented in Figure 4a. It can be observed that the addition of SLS, especially for concentrations higher than  $0.02 \text{ g L}^{-1}$ , led the cathodic branch to more negative potentials. However, the anodic branch, which corresponds to cobalt dissolution only, is dramatically reduced for SLS concentrations higher than  $0.02 \text{ g L}^{-1}$ , also indicating

inhibition of cobalt deposition. As the ratio of the anodic to cathodic areas of the voltammograms increase with the increase of SLS concentration it can be concluded that its effect is beneficial to the current efficiency, since its effect on the inhibition of hydrogen evolution should be greater than in the cobalt deposition reaction, resulting in higher current efficiency, as can be observed in Figure 4b.

Another factor to be considered in Figure 4b is the smaller growth in current efficiency for SLS concentrations higher than  $0.03 \text{ g L}^{-1}$ , indicating a kind of saturation of the additive effect on cobalt electrowinning. Jeffrey *et al.*<sup>15</sup> and Lu *et al.*<sup>20</sup> reported that SLS, a well-known surfactant, reduces the formation of pits on the deposit due to the presence of hydrogen bubbles on the cathode surface. Thus, the additive has been used as a stabilizing and anti-pitting agent, decreasing surface tension on the cathode, and facilitating the release of hydrogen bubbles.

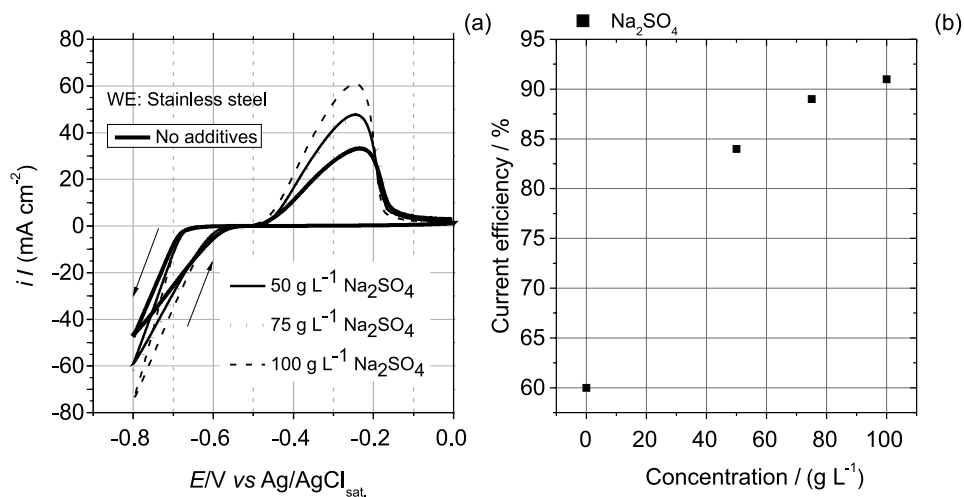


**Figure 3.** (a) Effect of sodium sulfate concentration on voltammograms and (b) current efficiency in a  $\text{CoSO}_4$  solution at  $60^\circ\text{C}$ , pH 4,  $60 \text{ g L}^{-1}$  of  $\text{Co}^{2+}$  ions and scan rate  $20 \text{ mV s}^{-1}$ .

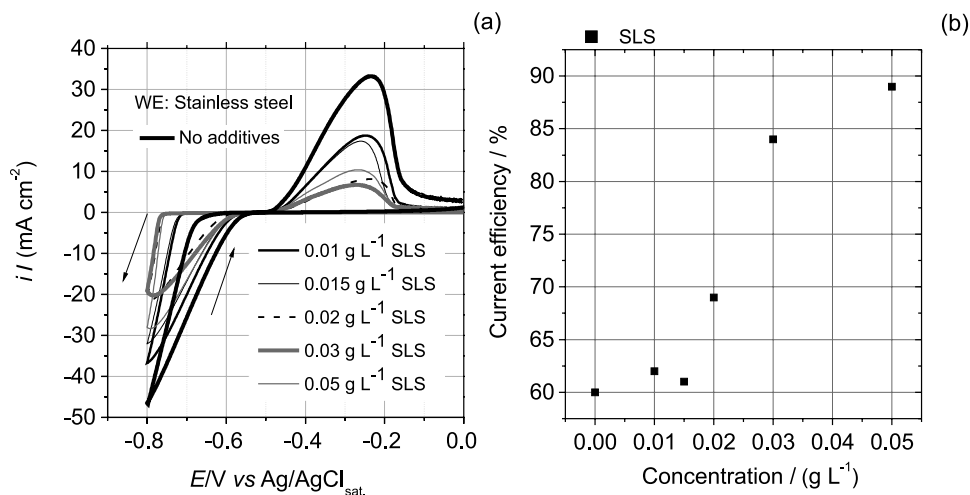


**Figure 4.** (a) Effect of sodium lauryl sulfate concentration on voltammograms and (b) current efficiency in a  $\text{CoSO}_4$  solution at  $60^\circ\text{C}$ , pH 4,  $60 \text{ g L}^{-1}$  of  $\text{Co}^{2+}$  ions and scan rate  $20 \text{ mV s}^{-1}$ .

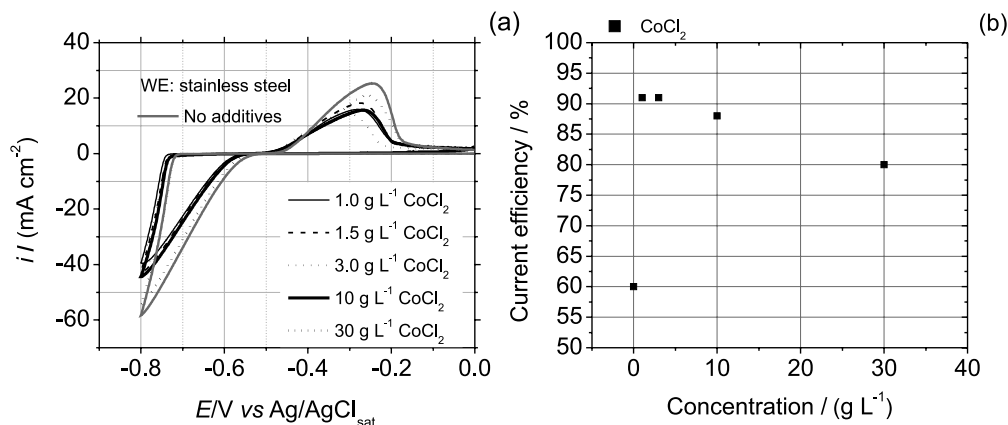


**Figure 5.** (a) Effect of chloride ion concentration on voltammograms and (b) current efficiency in a CoSO<sub>4</sub> solution at 60 °C, pH 4, 60 g L<sup>-1</sup> of Co<sup>2+</sup> ions concentration and scan rate 20 mV s<sup>-1</sup>.

### Effect of cobalt chloride concentration (CoCl<sub>2</sub>)

The effect of CoCl<sub>2</sub> concentration on the cyclic voltammograms for Co<sup>2+</sup> ions reduction on a stainless-steel electrode, followed by the dissolution of the deposited metal is presented in Figure 5a. It indicates that the increase of CoCl<sub>2</sub> concentration led the onset of electrodeposition to a more negative potential. The effect of CoCl<sub>2</sub> concentration on current efficiency is presented in Figure 5b. It can be observed that the presence of this additive at low concentrations (1 to 3 g L<sup>-1</sup>) does not interfere on current efficiency, which stands at 91%; but, at higher concentrations (10 to 30 g L<sup>-1</sup>), there is a significant decrease to 80%. According to Huang *et al.*,<sup>1</sup> the addition of chloride ions in the range of 0 to 30 g L<sup>-1</sup> decreases the current efficiency. Pradhan *et al.*<sup>18</sup> reported that the introduction of cobalt chloride (0-5000 mg dm<sup>-3</sup>) did not present any effect on current efficiency. Cobalt chloride was selected as an additive to avoid the presence of additional species in the solution.

Some complexes of cobalt with chloride ions can be formed in the electrolyte solution and deposited on the cathode, such as CoCl<sup>+</sup> ions. The cobalt chloride speciation diagram as a function of chloride ions concentration is presented in Figure 6. The speciation diagram was obtained by the Medusa software.<sup>33</sup> The equilibrium constants of ions and complex formation reactions (equations 7, 8, 9, 10) were obtained from Pan and Susak.<sup>34</sup>



According to Figure 6, at low chloride ion concentrations, it indicates the preferential formation of two cationic

species, Co<sup>2+</sup> and CoCl<sup>+</sup>. However, the predominant species for chloride ions additions up to 0.42 mol L<sup>-1</sup> is Co<sup>2+</sup> ions, corresponding to at least 90% of the cobalt ion concentration, while only 10% refers to CoCl<sup>+</sup> species.

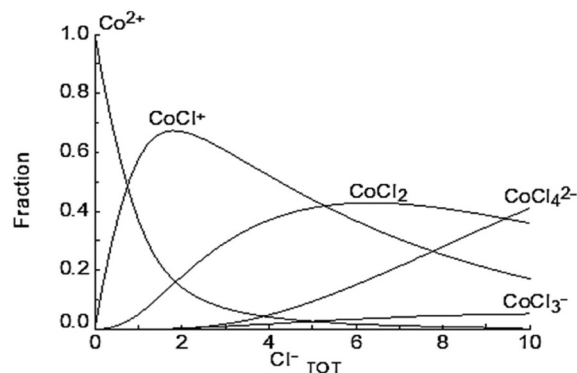


**Figure 6.** Speciation diagram of cobalt as a function of Cl<sup>-</sup> ions concentration in mol L<sup>-1</sup> on a condition with 60 g L<sup>-1</sup> of Co<sup>2+</sup>, pH 4, and 25 °C obtained by Medusa software.<sup>33</sup>

Another fact that can be mentioned about cobalt chloride electrolytes is the possible generation of chlorine gas on the anode. According to Mostafa *et al.*<sup>35</sup> studies, the electrogenerated chlorine species on the anode, arising from the electrolysis of highly saline water, was detected only for concentrations higher than 0.3 mol L<sup>-1</sup> of Cl<sup>-</sup> ions.

In relation to the electrowinning tests discussed in the next section, the maximum Cl<sup>-</sup> ions concentration used was 0.042 mol L<sup>-1</sup>. Therefore, there is no significant amount of chloride ions for chlorine evolution on the anode.

### Current efficiency (CE) values by CV and electrolysis tests

The current efficiency estimated by CV tests was compared with the current efficiency calculated by equation 5 in order to validate the estimation. Table 4

presents the current efficiency values of the CV and electrolysis tests for each additive and their concentrations.

**Table 4.** Current efficiency (CE) values obtained by CV and 6 h-electrolysis tests

| Concentration /<br>(g L <sup>-1</sup> ) | CE cyclic<br>voltammetry / % | CE 6 h of<br>electrolysis / % |
|---|------------------------------|-------------------------------|
| H <sub>3</sub> BO <sub>3</sub>          |                              |                               |
| 15                                      | 73                           | 80                            |
| 30                                      | 84                           | 91                            |
| 50                                      | 67                           | 74                            |
| Na <sub>2</sub> SO <sub>4</sub>         |                              |                               |
| 50                                      | 85                           | 78                            |
| 75                                      | 89                           | 82                            |
| 100                                     | 91                           | 84                            |
| SLS                                     |                              |                               |
| 0.01                                    | 62                           | 85                            |
| 0.03                                    | 84                           | 91                            |
| 0.05                                    | 89                           | 96                            |
| CoCl <sub>2</sub>                       |                              |                               |
| 1.0                                     | 91                           | 82                            |
| 10.0                                    | 87                           | 78                            |
| 30.0                                    | 80                           | 71                            |

SLS: sodium lauryl sulfate.

The different values of current efficiency can be attributed to the variation of current density in the cyclic voltammetry tests during both the cathodic and anodic potential scans. However, it is possible to observe that current efficiency follows the same trend for both analyses.

Co electrodeposition by CV tests occurs through the Co<sup>II</sup> species, since the scanning potential started at 0 V. Thus, there is no possibility of oxidation of Co<sup>II</sup> to Co<sup>III</sup>, since this oxidation only occurs at potentials around 1.84 V (*vs.* Ag/AgCl sat.). According to Rios-Reyes *et al.*,<sup>36</sup> the presence of the Co<sup>3+</sup> species in the cobalt electrodeposition is observed in the cyclic voltammograms as an initial

plateau before the reduction of the Co<sup>2+</sup> species. In relation to the voltammograms presented in this study, there was no evidence of interference by the Co<sup>3+</sup> species.

#### Statistical and morphological analysis of cobalt electrowinning tests

##### Factorial design for cobalt electrowinning

Current efficiency and specific energy consumption values are presented in Figures 7A and 7B in ascending order, respectively, while Table 5 shows these results in a factorial design matrix of experiments.

It can be observed that tests c and bc led to the highest current efficiencies, 96 and 95%, respectively, and the lowest specific energy consumption. Test c corresponds to an electrolytic solution with the maximum concentration of SLS, while the other additives were in their lowest level. In addition, the cyclic voltammetry experiments discussed in the previous section corroborate with c and bc tests, which indicate that the introduction of SLS up to 0.05 g L<sup>-1</sup> increased current efficiency to 89%.

Based on the results presented in Table 5, the maximum concentration of SLS (represented by “c” in Table 5) was the better-indicated condition for this electrowinning study since it renders the lowest specific energy consumption, 1.95 kWh kg<sup>-1</sup>, and highest current efficiency, 96%.

The effect of CoCl<sub>2</sub> and SLS interaction (represented by the “bc” in Table 5) was also beneficial to the current efficiency of long-duration electrolysis, reaching 95%. However, the effect of the maximum concentration of CoCl<sub>2</sub> (represented by “b” in Table 5) reached a current efficiency value of 82%. Thus, it is possible to conclude that the increase in current efficiency is mainly due to the addition of SLS.

Another additive to be discussed is H<sub>3</sub>BO<sub>3</sub>, a known buffer important to pH control at the interface cathode/

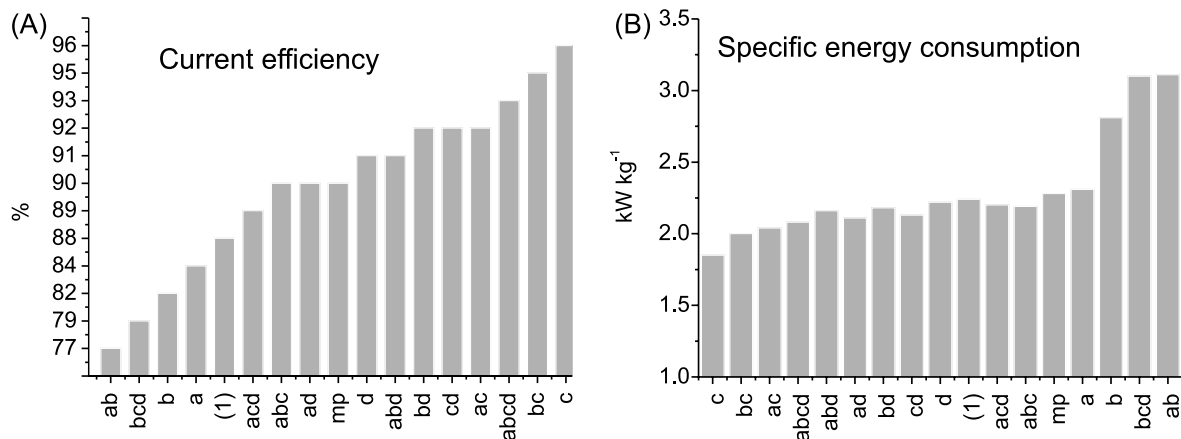


**Figure 7.** (A) Current efficiency and (B) specific energy consumption (kWh kg<sup>-1</sup>) of cobalt electrowinning tests from sulfate solution at 60 °C, pH 4, 200 A m<sup>-2</sup> and 60 g L<sup>-1</sup> of Co<sup>2+</sup> ions. I: Minimum concentration of additives; a: Na<sub>2</sub>SO<sub>4</sub> maximum concentration; b: CoCl<sub>2</sub> maximum concentration; c: SLS maximum concentration; d: H<sub>3</sub>BO<sub>3</sub> maximum concentration; mp: medium point.

**Table 5.** Influence of additives on cobalt electrowinning in a 2<sup>4</sup> factorial design with 2 replicas (subscripts 1 and 2) and 3 medium points

| Run label | CE <sub>1</sub> / % | CE <sub>2</sub> / % | SEC <sub>1</sub> / (kWh kg <sup>-1</sup> ) | SEC <sub>2</sub> / (kWh kg <sup>-1</sup> ) | A <sub>CE</sub> / % | A <sub>SEC</sub> / (kWh kg <sup>-1</sup> ) | SD <sub>CE</sub> / % | SD <sub>SEC</sub> / (kWh kg <sup>-1</sup> ) |
|-----------|---------------------|---------------------|--|--|---------------------|--|----------------------|---|
| (1)       | 89                  | 88                  | 2.19                                       | 2.24                                       | 88                  | 2.21                                       | 0.0007               | 0.02  |
| a         | 83                  | 85                  | 2.39                                       | 2.31                                       | 84                  | 2.35                                       | 0.010                | 0.04  |
| b         | 84                  | 81                  | 2.60                                       | 2.81                                       | 82                  | 2.70                                       | 0.016                | 0.10  |
| ab        | 75                  | 79                  | 3.44                                       | 3.11                                       | 77                  | 3.27                                       | 0.020                | 0.16  |
| c         | 95                  | 97                  | 2.04                                       | 1.85                                       | 96                  | 1.95                                       | 0.010                | 0.09  |
| ac        | 92                  | 95                  | 2.10                                       | 2.04                                       | 93                  | 2.07                                       | 0.016                | 0.03  |
| bc        | 94                  | 96                  | 2.08                                       | 2.00                                       | 95                  | 2.04                                       | 0.010                | 0.04  |
| abc       | 89                  | 92                  | 2.31                                       | 2.19                                       | 90                  | 2.25                                       | 0.016                | 0.06  |
| d         | 92                  | 91                  | 2.16                                       | 2.22                                       | 91                  | 2.19                                       | 0.0007               | 0.03  |
| ad        | 89                  | 91                  | 2.20                                       | 2.11                                       | 90                  | 2.15                                       | 0.01                 | 0.04  |
| bd        | 93                  | 92                  | 2.12                                       | 2.18                                       | 92                  | 2.15                                       | 0.0007               | 0.03  |
| abd       | 93                  | 90                  | 2.13                                       | 2.16                                       | 91                  | 2.14                                       | 0.015                | 0.01  |
| cd        | 92                  | 93                  | 2.17                                       | 2.13                                       | 92                  | 2.15                                       | 0.0005               | 0.02  |
| acd       | 90                  | 89                  | 2.27                                       | 2.20                                       | 89                  | 2.23                                       | 0.0005               | 0.03  |
| bcd       | 80                  | 79                  | 2.87                                       | 3.10                                       | 79                  | 2.98                                       | 0.0005               | 0.11  |
| abcd      | 94                  | 94                  | 2.08                                       | 2.08                                       | 94                  | 2.08                                       | 0                    | 0   |
| mp        | 92                  |                     | 2.26                                       | 2.28                                       | 90                  | 2.28                                       | 0.013                | 0.02  |
| mp        | 89                  |                     | 2.31                                       |  |                     |  |                      |   |
| mp        | 90                  |                     | 2.28                                       |  |                     |  |                      |   |

mp: medium point; CE: current efficiency; SEC: specific energy consumption; A<sub>CE</sub>: average current efficiencies; A<sub>SEC</sub>: average specific energy consumption of the replicas; SD<sub>CE</sub>: absolute standard deviation of the current efficiency; SD<sub>SEC</sub>: deviation of the specific energy consumption of the replicas ; 1: minimum concentration of additives; a: Na<sub>2</sub>SO<sub>4</sub> maximum concentration; b: CoCl<sub>2</sub> maximum concentration; c: SLS maximum concentration; d: H<sub>3</sub>BO<sub>4</sub> maximum concentration; mp: medium point; “a”, “b”, “c”, “d”, “ab”, “ac”, “bc”, “abc”, “ad”, “bd”, “abd”, “cd”, “acd”, “bcd” and “abcd” are the samples.

solution. At its higher level, the current efficiency and specific energy consumption obtained were respectively 91% and 2.19 kWh kg<sup>-1</sup> (represented by the “d” in Table 5). Their interaction with SLS additive, both at higher levels, also presents interesting results of current efficiency and energy consumption, 95% and 2.04 kWh kg<sup>-1</sup>, respectively.

To identify the absolute values of the standardized effects, the Pareto graph, presented in Figures 8a and 8b,

was obtained by the factorial design. Figure 8a indicated that the terms CD, C, AD and B showed a significant effect in descending order for the current efficiency response, while Figure 8b indicated the terms CD, B, AD and C for specific energy consumption.

The normal probability graph shown in Figures 9a and 9b was also obtained by the statistical analysis. Figures 9a and 9b indicate that the factorial design data fit the normal distribution, validating the empirical model of residuals.<sup>32</sup>

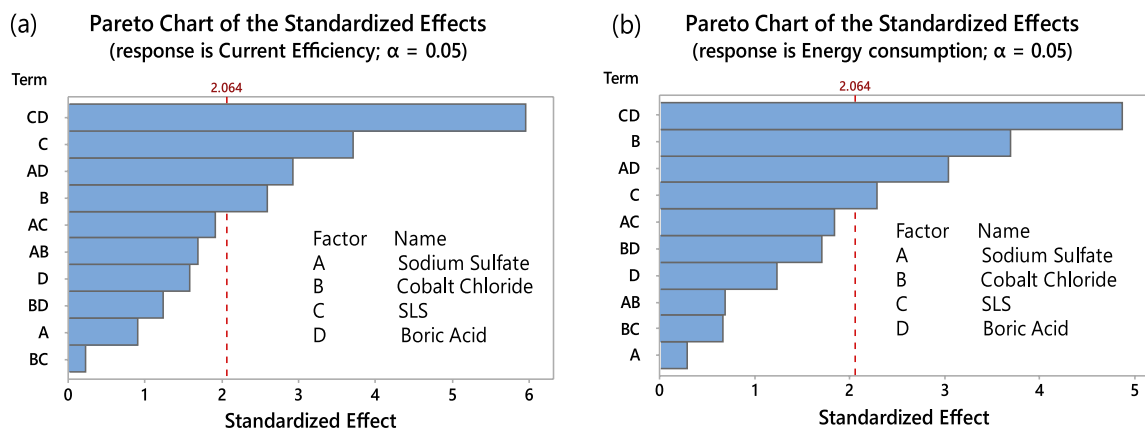


**Figure 8.** Pareto graph of standardized effects (a) current efficiency and (b) energy consumption of electrowinning tests under different additive concentrations in a CoSO<sub>4</sub> solution at 60 °C, pH 4, 200 A m<sup>-2</sup> and 60 g L<sup>-1</sup> of Co<sup>2+</sup> ions.

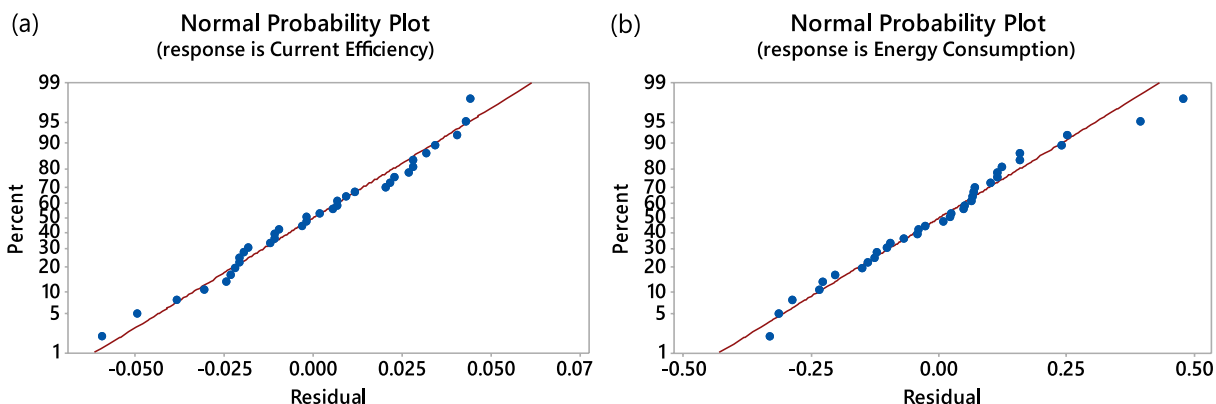


**Figure 9.** Normal probability graph of (a) current efficiency and (b) energy consumption of electrowinning tests under different additive concentrations in a  $\text{CoSO}_4$  solution at  $60^\circ\text{C}$ , pH 4,  $200\text{ A m}^{-2}$  and  $60\text{ g L}^{-1}$  of  $\text{Co}^{2+}$  ions.

Normalized regression equations were also obtained by the factorial design and indicated the factors and interactions that promoted significant effects on current efficiency and specific energy consumption. For current efficiency, C and AD tests led to an increase in current efficiency values, while CD and B led to a decrease. In contrast, for specific energy consumption, B and CD increased the energy consumption values, while C and AD decreased. The other factors and interactions were not statistically significant under the conditions of this study, as the  $p$ -values obtained were above 0.05, which indicates the non-significance of the results.<sup>32</sup>

$$\text{CE} = 0.86 - 0.21 \frac{B}{B_{\max}} + 0.25 \frac{C}{C_{\max}} + 0.28 \frac{AD}{A_{\max} D_{\max}} - 0.27 \frac{CD}{C_{\max} D_{\max}} \quad (11)$$

$$\text{EC} = 1.38 + 0.35 \frac{B}{B_{\max}} - 1.64 \frac{C}{C_{\max}} - 1.56 \frac{AD}{A_{\max} D_{\max}} + 1.48 \frac{CD}{C_{\max} D_{\max}} \quad (12)$$

The R-squared value is a statistical term that indicated

the adequacy of the statistical model for current efficiency and energy consumption since the values were 83.96 and 85.62%, respectively. The responses have a high predictive capacity of new observations, also validated by the empirical model of the residues (Figure 9).

To determine the accuracy of the AD interaction, the  $F$ -test values of residues for both responses were calculated with and without the presence of this interaction. According to Figure 10b, the area comprising the  $F$ -value with AD interaction is smaller, for CE and EC responses, than the statistical model without this interaction. Additionally, the  $R^2$  value for CE and EC responses was reduced to 75.01 and 63.43%, respectively; and it is possible to observe the non-occurrence of another significant factor in the model. Graber and co-workers<sup>37</sup> reported that sodium sulfate increases the boric acid solubility; this effect is due to the presence of sodium ions. Thus, the presence of sodium sulfate can enhance the effect of boric acid action on cobalt electrowinning. The  $F$ -test for CE and EC residues confirms the accuracy of statistical model since the  $p$ -values obtained for the regression model were less than 0.05. This provides a better fit than the intercept-only model.<sup>38</sup>

The optimized response graph shown in Figure 11 was obtained by the Derringer and Such desirability

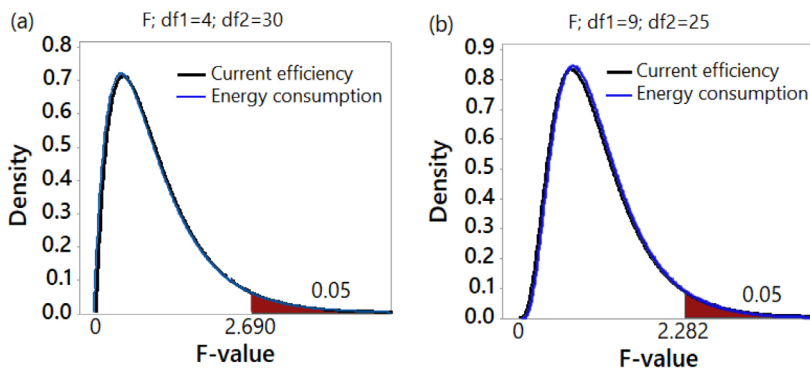


**Figure 10.** Distribution  $F$ -test of (a) current efficiency and energy consumption values with the AD interaction and (b) current efficiency and energy consumption values without the AD interaction.

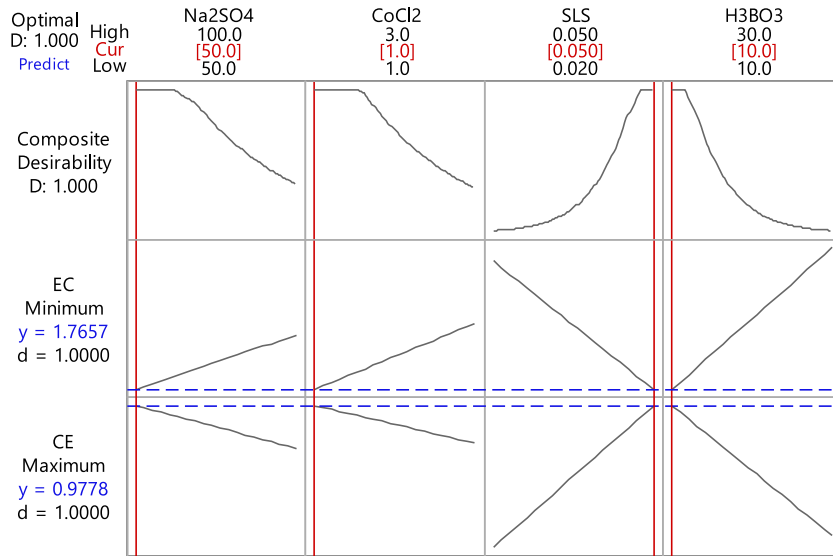


**Figure 11.** Optimized response graph for the conditions of additives concentrations on Co electrowinning from sulfate solution at 60 °C, pH 4, 200 A m<sup>-2</sup> and 60 g L<sup>-1</sup> of Co<sup>2+</sup> ions.

function and reports the optimized variables range of the response parameters.<sup>32</sup> In order to reduce the costs of cobalt electrowinning of this statistical study, current efficiency was maximized, while specific energy consumption was minimized. The  $y$  parameter in Figure 11 represented the current efficiency maximized and specific energy consumption minimized.

The composite desirability in Figure 11 indicates that the minimum concentration of Na<sub>2</sub>SO<sub>4</sub>, CoCl<sub>2</sub> and H<sub>3</sub>BO<sub>3</sub> additives led to high current efficiency and lower specific energy consumption, while the maximum concentration of SLS provided high current efficiency. The cobalt electrowinning result for this prediction method was achieved with test “c”.

**Morphological analysis of deposits obtained by cobalt electrowinning**

The macroscopic images of cobalt deposits are presented in Figure 12. They indicated that the “c” and “d” tests led to uniform cobalt deposits. Thus, the maximum concentration of SLS and H<sub>3</sub>BO<sub>3</sub> inhibited the H<sup>+</sup> ions reduction since there is no visible presence of pits on the cobalt deposit. It can also be observed that the presence of boric acid in its higher level led to clearer deposits, avoiding the formation of hydroxides on the electrode surface. However, its interaction with most of the additives in their higher level led to the rupture or wrapping of the deposits.

According to the literature, SLS is responsible for reducing surface tension at the electrode/electrolyte interface, providing a rapid release of hydrogen gas located on the cathode, reducing the formation of pits on the deposit.<sup>20,39</sup> However, the surface layer disruptions and warps of the

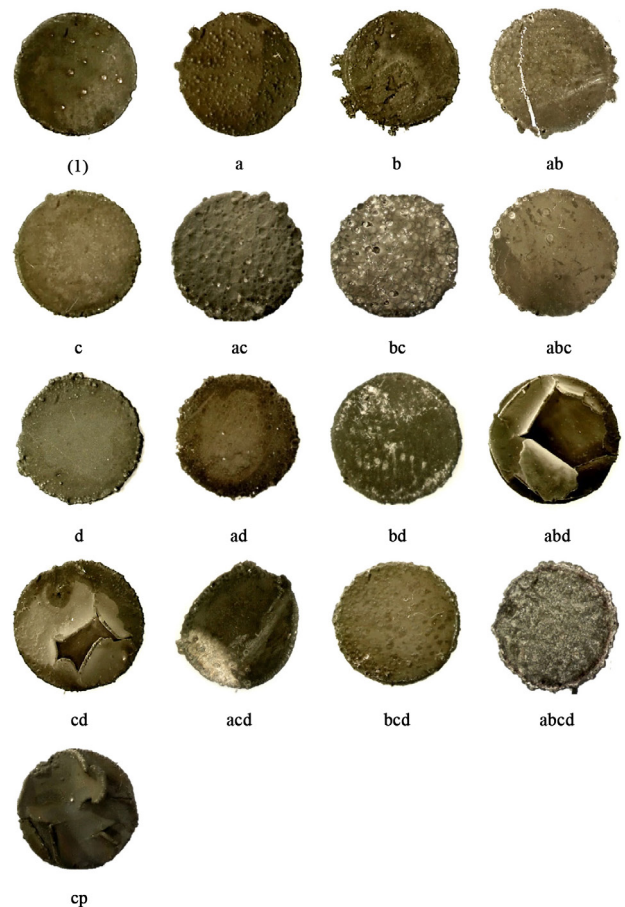


**Figure 12.** Images of cobalt deposits with 0.69 cm of diameter obtained by electrowinning under different additive concentrations in a CoSO<sub>4</sub> solution at 60 °C, pH 4, 200 A m<sup>-2</sup> and 60 g L<sup>-1</sup> of Co<sup>2+</sup> ions (magnitude: 30.00×). l: Minimum concentration of additives; a: Na<sub>2</sub>SO<sub>4</sub> maximum concentration; b: CoCl<sub>2</sub> maximum concentration; c: SLS maximum concentration; d: H<sub>3</sub>BO<sub>3</sub> maximum concentration; mp: medium point. The terms: “a”, “b”, “ab”, “c”, “ac”, “bc”, “abc”, “d”, “ad”, “bd”, “abd”, “cd”, “acd”, “bcd” and “abcd” are the samples.

deposited metal rounds on “cd”, “acd” and “bdc” deposits were identified in Figure 12. The combination of these additives in maximum concentrations promoted an increase in the internal tension of the deposit. Regarding the other deposits, the pits formations, and grains growth at the edge of the deposits were observed. The growth was caused by the higher local current density at the edge, which causes an increase in the reduction rate of the  $\text{Co}^{2+}$  ion.

The scanning electron microscopy images of cobalt deposits are presented in Figure 13. It can be observed that the main structure-modifying additives were  $\text{CoCl}_2$  (b), SLS (c),  $\text{H}_3\text{BO}_3$  (d), besides the interaction with  $\text{Na}_2\text{SO}_4 + \text{H}_3\text{BO}_3$  (ad).

The presence of chloride in its higher level led to the formation of a considerable amount of needles on the deposit, as can be seen in Figures 13, for samples (b), (bd), (abd) and (bdc). Pradhan *et al.*,<sup>18</sup> Alfantazi and Shakshouki,<sup>40</sup> and Soliz *et al.*<sup>41</sup> attributed those structures to the adsorption of chloride ions on the deposit surface.

The roughness was observed on the “a”, “b”, “cd”, “abd” and “bcd” deposit surfaces. For the “c” and “ad” deposits, the uniformity on the surface was verified with the

presence of elongated and compact structures. The presence of protuberances, identified on deposits “d”, “bd” and “abd”, can be attributed to hydroxides redissolution due to the presence of boric acid in its higher concentration level.

The presence of SLS in its higher concentration level led to the formation of compact structures as observed in samples “c”, “cd” and “bcd” deposits, when compared “a”, “d” and “bd”. In addition, the elongated structures caused by the presence of chloride ions observed on the “bd” deposit was reduced. According to Pissolati and Majuste,<sup>39</sup> organic compounds are important limiters of protuberances growth in nickel deposits since organic molecules are adsorbed on these sites, inhibiting their growth and producing more uniform deposits.

Regarding the purity of cobalt deposit, the energy dispersion spectroscopy results indicated that the more satisfactory condition (test “c”) presented some impurities such as sodium, boron, chlorine, sulfur, oxygen, and carbon, probably due to the entrapment of electrolyte during deposition. However, high concentrations of some impurities can affect some proprieties of cobalt deposits such as microhardness.<sup>39,42</sup>

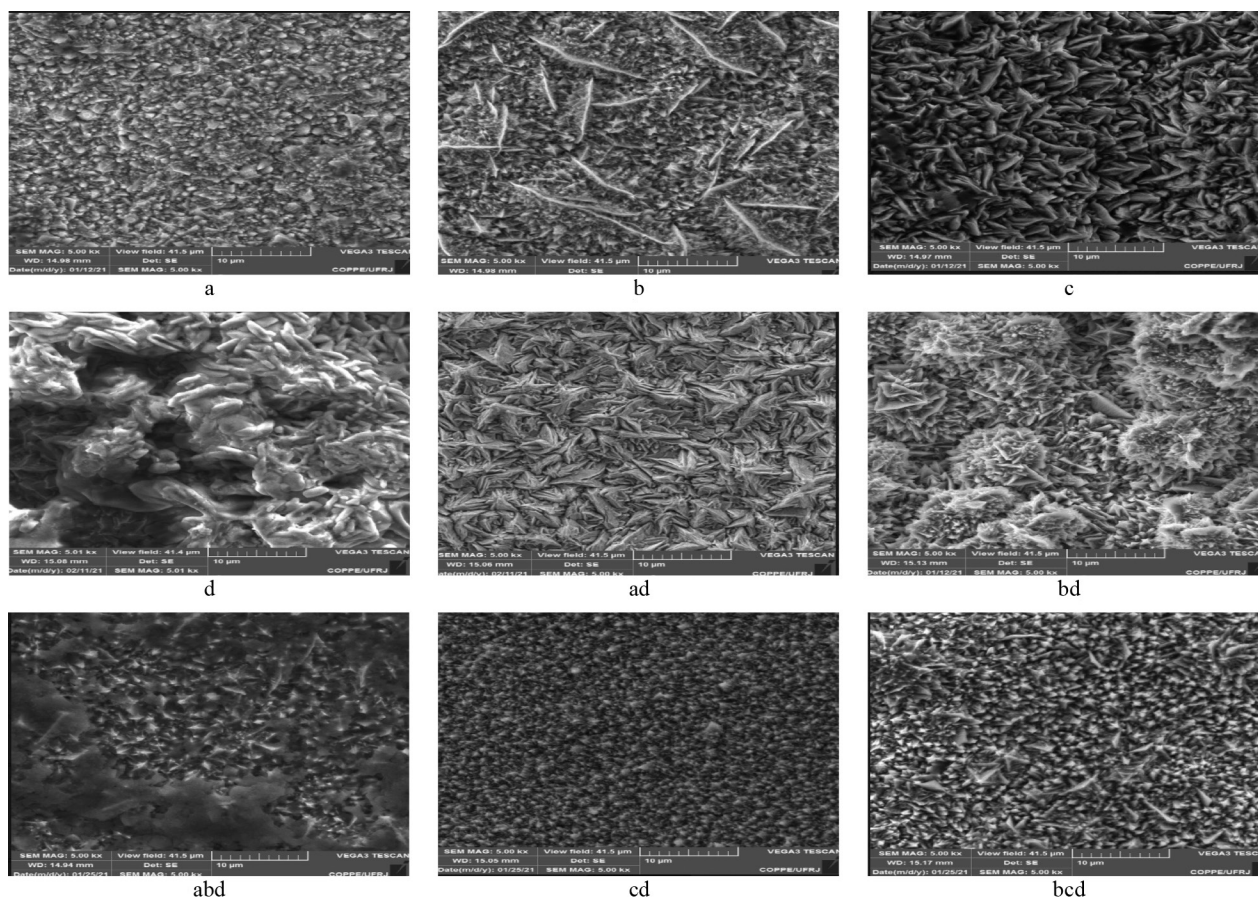


**Figure 13.** Scanning electron microscopy (SEM) images of deposits related to “a”, “b”, “c”, “d”, “ad”, “bd”, “abd”, “cd” and “bcd” experiments obtained by electrowinning under different additives concentrations in a  $\text{CoSO}_4$  solution at 60 °C, pH 4, 200  $\text{A m}^{-2}$  and 60  $\text{g L}^{-1}$  of  $\text{Co}^{2+}$  ions (SEM magnitude: 5.00kx). The terms “a”, “b”, “c”, “d”, “ad”, “bd”, “abd”, “cd” and “bcd” are the samples.

In this context, obtaining industrially acceptable metallic cobalt must have the characteristic of a uniform deposit, with no pits and a compact structure, as shown test “c”, to avoid the entrapment of impurities from the electrolyte. Furthermore, it is important to obtain an economically advantageous deposit with high current efficiency and low energy consumption.

## Conclusions

Cyclic voltammetry technique seems to be a fast and attractive technological option to investigate the effect of additives concentration most used on the cobalt electrowinning process. The effect of additives in cyclic voltammetry and long-duration tests of cobalt electrowinning were obtained based on experimental parameters suggested by this study.

Cyclic voltammograms indicated that the concentration ranges of 10 to 30 g L<sup>-1</sup> of boric acid, 50 to 100 g L<sup>-1</sup> of sodium sulfate, 0.02 to 0.05 g L<sup>-1</sup> of sodium lauryl sulfate and 1 to 3 g L<sup>-1</sup> of cobalt chloride on cobalt sulfate solutions led to highest results of estimated current efficiency. It can also be concluded that higher concentrations of boric acid, chloride cobalt and sodium lauryl sulfate raised cobalt nucleation overpotential and shifted the cobalt electrodeposition to more negative values.

From the factorial design results for cobalt electrowinning, based on cyclic voltammetry tests, the highest current efficiency (96%) and lowest specific consumption (1.95 kWh kg<sup>-1</sup>) can be achieved with 0.05 g L<sup>-1</sup> of sodium lauryl sulfate, 10 g L<sup>-1</sup> of boric acid, 50 g L<sup>-1</sup> sodium sulfate and 1.0 g L<sup>-1</sup> of chloride cobalt in an electrolytic cell with 60 g L<sup>-1</sup> of Co<sup>2+</sup> (CoSO<sub>4</sub>·7H<sub>2</sub>O), at 60 °C, pH 4 and current density of 200 A m<sup>-2</sup> (test “c”).

The macroscopic and microscopic analysis indicated that the best condition obtained from the factorial design (test “c”) led to smooth metallic deposits without evident pits and other defects. Besides, it can be concluded that higher concentrations of boric acid led to clearer deposits and an increase of protuberances. Also, the higher concentration of sodium lauryl sulfate provides reduction of pits on the deposits.

## Supplementary Information

Supplementary information is available free of charge at <http://jbcs.sbc.org.br> as a PDF file.

## Acknowledgments

The authors would like to acknowledge Instituto

Tecnológico Vale (ITV), and National Council for Scientific and Technological Development (CNPq, grant No. 304018/2020-1) for the support.

## References

- Huang, J. H.; Kargl-Simard, C.; Alfantazi, A. M.; *Can. Metall. Q.* **2004**, *43*, 163. [Crossref]
- Dehaine, Q.; Tijsseling, L. T.; Glass, H. J.; Törmänen, T.; Butcher, A. R.; *Miner. Eng.* **2021**, *160*, 106656. [Crossref]
- U.S. Geological Survey (USGS); *Mineral Commodity Summaries 2021*; U.S. Geological Survey: Reston, 2021, p. 200. [Link] accessed in March 2023
- Crundwell, F. K.; du Preez, N. B.; Knights, B. D. H.; *Miner. Eng.* **2020**, *156*, 106450. [Crossref]
- Alves Dias, P.; Blagoeva, D.; Pavel, C.; Arvanitidis, N.; *Cobalt: Demand-Supply Balances in the Transition to Electric Mobility*; Publications Office of the European Union: Petten, The Netherlands, 2018, ch. 2. [Crossref]
- Li, M.; Lu, J.; *Science* **2020**, *367*, 979. [Crossref]
- Zhang, T.; Bai, Y.; Shen, X.; Zhai, Y.; Ji, C.; Ma, X.; Hong, J.; *Int. J. Life Cycle Assess.* **2021**, *26*, 1198. [Crossref]
- Mansur, M. B.; Guimarães, A. S.; Petranková, M.; *Miner. Process. Extr. Metall. Rev.* **2021**, *43*, 489. [Crossref]
- Chen, Z.; Zhang, L.; Xu, Z. J.; *J. Cleaner Prod.* **2020**, *275*, 122841. [Crossref]
- Stinn, C.; Allanore, A.; *Electrochem. Soc. Interface* **2020**, *29*, 44. [Crossref]
- Zhang, Y.; Zhao, H.; Qian, L.; Sun, M.; Lv, X.; Zhang, L.; Petersen, J.; Qiu, G.; *Miner. Eng.* **2020**, *158*, 106586. [Crossref]
- Kongstein, O. E.; Haarberg, G. M.; Thonstad, J.; *J. Appl. Electrochem.* **2007**, *37*, 669. [Crossref]
- Espinoza, E. M.; Clark, J. A.; Soliman, J.; Derr, J. B.; Morales, M.; Vullev, V. I.; *J. Electrochem. Soc.* **2019**, *166*, H3175. [Crossref]
- Patnaik, P.; Padhy, S. K.; Tripathy, B. C.; Bhattacharya, I. N.; Paramguru, R. K.; *Trans. Nonferrous Met. Soc. China* **2015**, *25*, 2047. [Crossref]
- Jeffrey, M. I.; Choo, W. L.; Breuer, P. L.; *Miner. Eng.* **2000**, *13*, 1231. [Crossref]
- Lupi, C.; Pilone, D.; *Miner. Eng.* **2001**, *14*, 1403. [Crossref]
- Crittelli, R. A. J.; Sumodjo, P. T. A.; Bertotti, M.; Torresi, R. M.; *Electrochim. Acta* **2018**, *260*, 762. [Crossref]
- Pradhan, N.; Singh, P.; Tripathy, B. C.; Das, S. C.; *Miner. Eng.* **2001**, *14*, 775. [Crossref]
- Zhou, J.; Wang, S.; Song, X.; *Trans. Nonferrous Met. Soc. China* **2016**, *26*, 1706. [Crossref]
- Lu, J.; Dreisinger, D.; Glück, T.; *Hydrometallurgy* **2018**, *178*, 19. [Crossref]
- Venkatesan, P.; Sun, Z. H. I.; Sietsma, J.; Yang, Y.; *Sep. Purif. Technol.* **2018**, *191*, 384. [Crossref]

22. Matsushima, J. T.; Trivinho-Strixino, F.; Pereira, E. C.; *Electrochim. Acta* **2006**, *51*, 1960. [Crossref]
23. Santos, J. S.; Matos, R.; Trivinho-Strixino, F.; Pereira, E. C.; *Electrochim. Acta* **2007**, *53*, 644. [Crossref]
24. Lu, J.; Yang, Q.-h.; Zhang, Z.; *Trans. Nonferrous Met. Soc. China* **2010**, *20*, s97. [Crossref]
25. Santos, J. S.; Trivinho-Strixino, F.; Pereira, E. C.; *Surf. Coat. Technol.* **2010**, *205*, 2585. [Crossref]
26. Tripathy, B. C.; Singh, P.; Muir, D. M.; *Metall. Mater. Trans. B* **2001**, *32*, 395. [Crossref]
27. Passos, F. A. C. M.; dos Santos, I. D.; Dutra, A. J. B.; *Miner. Process. Extr. Metall. Rev.* **2022**. [Crossref]
28. Sharma, I. G.; Alex, P.; Bidaye, A. C.; Suri, A. K.; *Hydrometallurgy* **2005**, *80*, 132. [Crossref]
29. Elsherief, A. E.; *J. Appl. Electrochem.* **2003**, *33*, 43. [Crossref]
30. *Origin*, version 9.0; OriginLab Corporation, Northampton, MA, USA, 2019.
31. *Minitab*, version 19, Minitab Inc., State College, PA, USA, 2019. [Link] accessed in March 2023
32. Montgomery, D. C.; *Design and Analysis of Experiments*, vol. 1, 6<sup>th</sup> ed.; Wiley: New Jersey, USA, 2004.
33. Puigdomenech, I.; *Chemical Diagrams (Medusa-Hydra), Visual Basic 6*; Royal Institute Technology, Sweden, 2010.
34. Pan, P.; Susak, N. J.; *Geochim. Cosmochim. Acta* **1989**, *53*, 327. [Crossref]
35. Mostafa, E.; Reinsberg, P.; Garcia-Segura, S.; Baltruschat, H.; *Electrochim. Acta* **2018**, *281*, 831. [Crossref]
36. Rios-Reyes, C. H.; Mendoza-Huizar, L. H.; Reyes-Cruz, V. E.; Veloz Rodríguez, M. A.; *Quim. Nova* **2013**, *36*, 97. [Crossref]
37. Alavia, W.; Lovera, J.; Graber, T. A.; *Fluid Phase Equilib.* **2015**, *398*, 63. [Crossref]
38. Ferreira, A. S.; Mansur, M. B.; *Process Saf. Environ. Prot.* **2011**, *89*, 172. [Crossref]
39. Pissolati, N. C.; Majuste, D.; *Hydrometallurgy* **2018**, *175*, 193. [Crossref]
40. Alfantazi, A. M.; Shakshouki, A. J.; *Electrochem. Soc.* **2002**, *149*, C506. [Crossref]
41. Soliz, A. C.; Alfaro, C.; Cáceres, L.; Guzman, D.; *Matéria* **2021**, *26*, e12941. [Crossref]
42. Mahdavi, S.; Allahkaram, S. R.; *Trans. Nonferrous Met. Soc. China* **2018**, *28*, 2017. [Crossref]

Submitted: February 14, 2023

Published online: April 6, 2023

